



Effective seeding strategy using flat type poly (vinyl alcohol) cryogel for anammox enrichment

Minkyu Choi ^{a,b}, Kyungjin Cho ^a, Seockheon Lee ^a, Yun-Chul Chung ^a, Joonhong Park ^{b,**}, Hyokwan Bae ^{c,*}

^a Center for Water Resource Cycle Research, Korea Institute of Science and Technology (KIST), 5 Hwarang-ro 14-gil, Seongbuk-gu, Seoul 02792, Republic of Korea

^b Department of Civil and Environmental Engineering, Yonsei University, 50 Yonsei-ro, Seodaemun-Gu, Seoul 03722, Republic of Korea

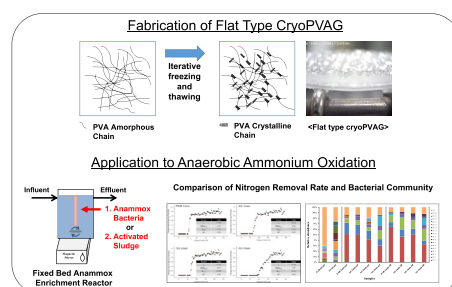
^c Department of Civil and Environmental Engineering, Pusan National University, 63 Busandaehak-ro, Geumjeong-Gu, Busan 46241, Republic of Korea



HIGHLIGHTS

- Flat type cryoPVAG was utilized for anammox enrichment.
- Four anammox reactors with different inocula and thicknesses were used.
- The start-up period of anammox reactors was evaluated by a modified Gompertz model.
- Substrate diffusion limitation of cryoPVAG was verified at different gel thicknesses.
- *Candidatus Brocadia sinica* was the predominant species after anammox enrichment.

GRAPHICAL ABSTRACT



ARTICLE INFO

Article history:

Received 15 January 2018

Received in revised form

29 March 2018

Accepted 6 April 2018

Available online 13 April 2018

Keywords:

Anaerobic ammonium oxidation

Poly (vinyl alcohol) cryogel

Inoculum source

Substrate diffusion limitation

Illumina MiSeq

ABSTRACT

In this study, anammox enrichment reactors were operated using flat type poly (vinyl alcohol) cryogel (cryoPVAG) with precultured anammox bacteria (PAB) and activated sludge (AS) from an anoxic tank of the A2O process to evaluate the effect of different seeding sources on anammox enrichment. In addition, cryoPVAGs with different thicknesses (1, 2, and 3 mm) were used to investigate the effects of the thickness on anammox enrichment. The regression analysis with a modified Gompertz model showed that the start-up period of the anammox enrichment using PAB inoculum was approximately 14 days earlier than that of AS inoculum at a nitrogen loading rate of approximately $1 \text{ kg-N m}^{-3} \text{ day}^{-1}$. Substrate diffusion was limited in 3-mm cryoPVAG with respect to trend in nitrogen removal rate. Quantitative PCR analysis indicated that in the initial phase, the 16S rRNA gene copy numbers of anammox microorganism in cryoPVAG were significantly different according to the seeding source, but finally converged to a similar level after anammox enrichment. The anammox reaction was initially promoted by cryoPVAG. Next, anammox biomass detached from cryoPVAG and enriched in the bulk phase to maximize NRR. Illumina MiSeq sequencing revealed that *Candidatus Brocadia sinica* led to the active anammox reaction, and its relative abundance decreased with increasing gel thickness.

© 2018 Elsevier Ltd. All rights reserved.

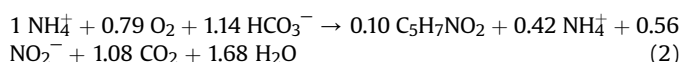
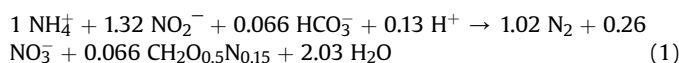
* Corresponding author.

** Corresponding author.

E-mail addresses: parkj@yonsei.ac.kr (J. Park), hyokwan.bae@pusan.ac.kr (H. Bae).

1. Introduction

Eutrophication in water environments derived from excessive nitrogen disposal is a serious environmental problem (Smith et al., 1999). As a solution for nutritional pollution, conventional biological nitrogen removal (BNR) consisting of nitrification and denitrification is the preferred biological technology for use in wastewater treatment plants. However, these BNR processes have limitations, such as the requirement for excessive aeration for nitrification and an external carbon source for denitrification. Anaerobic ammonium oxidation (anammox) shown in Eq. (1) is a promising alternative solution as a cost-effective nitrogen removal process (Mulder et al., 1995; Van de Graaf et al., 1995; Strous et al., 1998). To ensure successful nitrogen removal, stable partial nitritation (PN) is required prior to the anammox process as a pretreatment rather than complete nitrification (Eq. (2)).



Compared to conventional BNR processes, aeration is reduced by 56.8% in the PN process based on the stoichiometric calculation, and an external carbon source is not required because the PN-anammox process is completely autotrophic. Additionally, the reduction in CO₂ emission is another advantage (Tian et al., 2015). However, anammox bacteria have a long doubling time of 11 days and low sludge output of 0.11 g volatile suspended solids (VSS) per g NH₄⁺-N (Van Dongen et al., 2001). The slow growth rate of anammox bacteria positively affects the treatment of excess sludge production, but the start-up period for activating anammox reaction significantly increases.

The technique for securing a large amount of anammox bacteria is important for promoting the anammox reaction and reducing the start-up period in wastewater treatment processes. Diverse types of bioreactors with efficient retention of anammox bacteria have been designed. A batch system using suspended cells is used to initiate the anammox reaction and enrich anammox bacteria under anoxic conditions, however, the slow growth yield prevented massive cultivation (Van de Graaf et al., 1995). More suitable reactors in continuous mode have been developed using suspended sludge and attached-growth biomass including sequencing batch reactor, membrane bioreactor, up-flow anaerobic sludge blanket reactor, fixed bed reactor, rotating biological contactor and upflow biofilter (Strous et al., 1998; Egli et al., 2001; Fux et al., 2004; Trigo et al., 2006; Jin et al., 2008; Bae et al., 2016). Previous studies have also attempted to enrich anammox activity by using conventional activated sludge (AS), which is a useful seeding source when pre-cultured anammox bacteria (PAB) are not available for start-up (Gutwiński et al., 2016; Cho et al., 2017).

Among anammox enrichment systems, whole cell immobilization is a promising approach to overcome the slow growth rate of anammox bacteria. Whole cell immobilization techniques are advantageous because they show enhanced retention of biomass by preventing washout through easy solid-liquid separation and consequent reduction in the lag period (Chen et al., 1996; Hsia et al., 2008). Poly (vinyl alcohol) (PVA) has been widely used for whole cell immobilization because it is relatively inexpensive and has excellent tensile strength without causing toxicity to the microorganism (Hsia et al., 2008; Chou et al., 2012). Particularly, PVA-sodium alginate (PVA-SA) gel beads using bifunctional reagent of boric acid (B(OH)₃) and calcium chloride (CaCl₂) are representative gel material for environmental remediation. Using PVA-boric acid

reaction, boric acid acts as the crosslinker, and four molecules of PVA are linked with boron. Consequently, monodiol type of gel lattice by PVA-boric acid is produced (Bae et al., 2017; Tang et al., 2017). PVA-SA gel beads have been also used for anammox enrichment (Chen and Lin, 1994; Ali et al., 2015; Bae et al., 2017). However, because a dense layer is formed on the surface during the PVA-SA fabrication process, gas permeability is decreased and the gel expands by the accumulation of gas contents produced by microorganisms (Chen et al., 1996; Chen and Houg, 1997).

From this perspective, PVA cryogel (cryoPVAG) is attractive material for wastewater treatment including in the anammox process due to the enhanced gas permeability and structural stability (Asano et al., 1992; Sheng et al., 2008; Magrí et al., 2012). CryoPVAG is fabricated by gelation through repetitive freezing and thawing. Freezing process initiates the phase separation of PVA solution into the frozen solvent crystal (i.e., water crystal) and unfrozen liquid microphase of PVA. The gel-forming constituents are concentrated in the unfrozen liquid microphase while accelerating the rate of PVA cryogel formation. After thawing, the water crystals melt but the formed gel remains. As a result, macroporous hydrogel, i.e., cryogel, is produced (Lozinsky et al., 2003; Lozinsky and Okay, 2014). In terms morphology, only the cube-type of cryoPVAG has been used previously. In this study, flat type cryoPVAG was applied to start-up the anammox process. Effective diffusion of NH₄⁺ and NO₂⁻ was limited by up to 1.3 mm (Ni et al., 2009). However, a typical PVA-SA gel bead is 3–5 mm in diameter, indicating that it has a large inactive area, also known as a dead space (Zhang and Ye, 2011; Ali et al., 2015; Bae et al., 2015). Thus, we predicted that minimizing the thickness of the cryoPVAG may rapidly increase anammox activity, even with less seeding source. In addition, stable structure of a flat type cryoPVAG was expected to prevent abrasion and loss of PVA gel during anammox enrichment.

In this study, flat type cryoPVAGs with thicknesses of 1, 2 and 3 mm were applied in anammox enrichment to determine the optimum thickness. Two seeding sources of PAB and AS were used. Nitrogen removal performance was evaluated according to seeding source and thickness of the cryoPVAG. A continuous reactor was inoculated with fixed bed cryoPVAG with minimized packing ratio. Real-time quantitative polymerase chain reaction (qPCR) was applied to verify the growth of total and anammox bacteria, and changes in bacterial community structure were identified by high-throughput sequencing method.

2. Materials and methods

2.1. Seeding sludge

PAB were obtained from an up-flow continuous bioreactor and AS was taken from a domestic wastewater treatment plant in Daejeon, South Korea (Bae et al., 2010a). The dominant anammox bacteria species of PAB and AS was *Candidatus Jettenia* sp. in the phylum Planctomycetes (Bae et al., 2017). The inoculum of PAB was composed of 63.2% and 36.8% of VSS and fixed suspended solids (FSS), respectively; AS consisted of 79.9% and 20.1% of VSS and FSS, respectively. Two inoculum sources were homogenized using a homogenizer (IKA, T18 digital ULTRA-TURRAX®, Staufen, Germany) including a dispersing element (S18N-10G). The VSS concentration of inoculum injected into the flat type cryoPVAG were 5271.7 ± 498.6 and 7116.7 ± 40.4 mg-VSS L⁻¹ of PAB and AS, respectively.

2.2. Preparation of flat type cryoPVAG

The cryoPVAG was fabricated using a 10% PVA solution. The 10%

PVA solution showed the stable mechanical strength of the cryoPVAG (Magrí et al., 2012). In detail, PVA solution containing 20% PVA was autoclaved at 121 °C for 30 min to dissolve PVA particles completely, followed by cooling of this solution to 37 °C. The same volume of each homogenized PAB and AS solution was mixed with PVA solution. Finally, a 10% PVA mixture was obtained. The PVA mixture was poured into rectangular steel plate frames (60 × 120 mm) with heights of 1, 2 and 3 mm. Each steel plate frame was stored at –20 °C for 24 h to initiate phase separation of PVA solution followed by thawing at room temperature (23–25 °C) for 1 h. The freezing and thawing process was repeated two additional times to enhance mechanical strength. The prepared flat type cryoPVAG was rinsed with sterilized water and mounted on an acrylic frame to be fixed in the bioreactor. The swelling property of the cryoPVAG was tested after the washing. The thicknesses of 0.97 ± 0.013, 2.1 ± 0.044 and 3.1 ± 0.051 mm were marginally increased to 1.04 ± 0.030, 2.15 ± 0.013 and 3.12 ± 0.071 mm, respectively. Therefore, the swelling was negligible in this study.

2.3. Experimental set-up for anammox enrichment

To enrich the anammox bacteria, four identical lab-scale bioreactors with a working volume of 0.29 L were operated for 240 days. CryoPVAGs were provided in four types: PAB inoculum with a thickness of 1 mm (PAB-1mm) and AS inoculum with thicknesses of 1, 2 and 3 mm (AS-1mm, AS-2mm and AS-3mm). Acrylic frames mounted with cryoPVAG were inserted into each continuous bioreactor. The packing ratio (i.e., the ratio of cryoPVAG volume to total reactor volume) was 1.72%. All bioreactors were designed to prevent the intrusion of ambient air with by sealing. While the cryoPVAG was firmly fixed, the bulk phase of bioreactors was agitated at the bottom by a rotating magnetic stirrer (Misung Scientific Co., Ltd. Kyunggi-do, Republic of Korea) at 500 rpm. Temperature was maintained at 35 °C by using a constant temperature chamber (Sejong Scientific Co., Gyeonggi-do, Republic of Korea). The pH levels of the influent were 7.8 ± 0.15. The hydraulic retention time was adjusted to 2.52 h.

Synthetic wastewater was composed of ammonium nitrogen (NH_4^+-N) as an electron donor, nitrite nitrogen (NO_2^--N) as an electron acceptor, bicarbonate (HCO_3^-) as an inorganic carbon source and small amount of trace nutrients. NH_4^+-N , NO_2^--N and HCO_3^- in the influent were supplied in the form of $(\text{NH}_4)_2\text{SO}_4$, NaNO_2 and NaHCO_3 . Other substances are described in Table S1. In all bioreactors, influent NH_4^+-N and NO_2^--N concentrations were fixed at 50 mg L⁻¹ and 66 mg L⁻¹, respectively, and the nitrogen loading rate (NLR) was maintained at 1.16 ± 0.064 kg-N m⁻³ day⁻¹. An exponential increase in the nitrogen removal rate (NRR) was observed at the fixed NLR. An integrated Gompertz model was applied to analyze the characteristics of anammox enrichment according to different cryoPVAGs (Eq. (3)) (Jin et al., 2013).

$$\text{NRR} = \text{NRR}_{\text{max}} \times \exp \left[- \exp \left(\frac{\text{R}_{\text{max}} e}{\text{NRR}_{\text{max}}} (\lambda - t) + 1 \right) \right] \quad (3)$$

where NRR is the nitrogen removal rate (kg-N m⁻³ d⁻¹); NRR_{max} is the maximum NRR (kg-N m⁻³ d⁻¹); R_{max} is the acceleration of nitrogen removal rate; λ is the lag time of the bioreactor (day); and t is the elapsed time (day). The calculated values of NRR_{max} , λ and R_{max} from the Gompertz model were fitted by the non-linear regression program Origin 8.0 software (OriginLab®, Northampton, MA, USA).

After enrichment of anammox bacteria, the incubated cryoPVAG was removed from the reactors and blank cryoPVAG was added to identify the contribution of anammox bacteria immobilized in the PVAG and suspended in the bulk phase to NRR after enrichment for

an additional 15 days.

2.4. Quantitative PCR (qPCR)

Genomic DNA was extracted from cryoPVAGs and suspended biomass (SB) under the steady-state condition (day 240) using the MoBio Power Soil DNA Kit (MoBio Laboratories, Carlsbad, CA, USA) following manufacturer's instructions. qPCR was performed to quantify the population of total and anammox bacteria. The reaction mixture (20 µL) for qPCR was prepared as follows: 10 µL of 2 × TaqMan® Fast Advanced Master Mix (Applied Biosystems, Foster City, CA, USA) in sterilized distilled water was mixed with each primer and probe with at the appropriate concentration for target bacteria, and then 1 µL of DNA template was added. The detailed information regarding the concentrations of primers and probe and amplification process of PCR for total bacteria and anammox bacteria are described in Tables S2 and S3 (Nadkarni et al., 2002; Bae et al., 2010b). qPCR analysis was performed using a thermal cycler (ABI Prism 7300 sequence detection system, Applied Biosystems). Each qPCR sample was tested in triplicate. The number (16 rRNA gene copies) of total bacteria and anammox microorganisms was estimated from multiplying the DNA concentrations of the qPCR results (copies mL⁻¹) by the volume of gel and bulk phase (mL).

2.5. Illumina MiSeq sequencing

An Illumina MiSeq platform (Illumina, San Diego, CA, USA) was applied to investigate the bacterial community structure. Bacterial 16S rRNA genes in the V3 to V4 region were amplified using universal primers, i.e., 341F and 785R (Klindworth et al., 2013). The library construction, sequencing process and data processing of PCR products were conducted by Macrogen Inc. (Seoul, Korea). From the resulting sequences, operational taxonomic units (OTUs) with at least 97% sequence similarity were generated using the cluster database at high identity with tolerance method. The bacterial OTUs were used to match the closest reported OTUs using the National Center for Biotechnology Information blast database. Good's coverage was generated by MOTHUR for each sample. Good's coverage values (Table S4) were greater than 99.8% in all samples, indicating that there was a satisfactory number of sequences to characterize the microbial community (Kowalchuk et al., 2004).

2.6. Analytical methods

NH_4^+-N was measured as described by Kjeldahl method (Kjeltec 2300, Foss Tecator, Hilleroed, Denmark). NO_2^--N and VSS were analyzed using standard methods; to measure VSS concentration, GF/C filter papers (Whatman, Maidstone, UK) with 0.45 µm pore size were used. Nitrate nitrogen (NO_3^--N) was measured using a HACH kit (program 351 for nitrate, HACH, Loveland, CO, USA). pH values were determined with a pH meter (Accumet® Basic AB15 Plus pH Meter, Thermo Fisher Scientific, Waltham, MA, USA).

3. Results and discussion

3.1. Increase in anammox activity

NLR and NRR of the lab-scale bioreactors are shown in Fig. 1. During the initial 54 days, total nitrogen removal was not observed in all four bioreactors. After 55 days, PAB-1mm anammox exhibited the shortest lag period in the anammox reaction. Fourteen days later, the maximum NRR was achieved, and the average NRR and nitrogen removal efficiency were maintained at 0.93 ± 0.067 kg-N

$\text{m}^{-3} \text{day}^{-1}$ and $79.46 \pm 0.024\%$, respectively. The AS-1mm and AS-2mm bioreactors showed an identical lag period of 69 days, which is longer than the 55 days of PAB-1mm. After 24 days, the maximum NRRs of the two bioreactors were $0.95 \text{ kg-N m}^{-3} \text{ day}^{-1}$ with small statistical deviations of ± 0.075 and ± 0.064 for AS-1mm and AS-2mm, respectively. As the latest start-up, the initial anammox activity of the AS-3mm was observed on day 93 when the maximum NRRs of the other reactors were already achieved. In addition, the additional operational period to achieve the maximum NRR of $0.97 \pm 0.027 \text{ kg-N m}^{-3} \text{ day}^{-1}$ was also the longest for the AS-3mm, i.e., 74 days, compared to the other reactors.

Changes in nitrogen compounds are shown in Fig. 2. After anammox activity was stabilized, the average effluent concentrations of NH_4^+-N and NO_2^--N were maintained below 1 and 5 mg L^{-1} , respectively, in all bioreactors. In the anammox reaction, NH_4^+-N and NO_2^--N were consumed at a ratio of 1: 1.41 ± 0.021 under the steady state for the four bioreactors. In addition, the NO_3^- concentration was maintained between 21.0 and 21.7 mg L^{-1} . As a result, the $\text{NH}_4^+:\text{NO}_3^-$ ratio was calculated as 1: 0.39 ± 0.019 , which is approximately 50% greater than the theoretical stoichiometric ratio. Commonly, the representative anammox stoichiometric ratio of 1:1.32:0.26 is acceptable (Strous et al., 1998). However, the stoichiometric ratio is different according to dominant anammox species, and sometimes high NO_3^- -N production is observed (Isaka et al., 2007; Yamamoto et al., 2008). Furthermore, the culture medium of this study contained only inorganic carbon source as NaHCO_3 without organic carbon source. Thus, it is expected that heterotrophic denitrification was limited.

Previous studies reported that PVA-SA has an effective entrapment matrix that minimizes the lag period for anammox activity (Quan et al., 2011; Zhu et al., 2014; Ali et al., 2015; Cho et al., 2017). Cube-type cryoPVAG was also used for anammox enrichment (Magrı et al., 2012). Compared to anammox processes using other whole cell immobilization techniques, the anammox enrichment results in this study showed a relatively long lag period (Table 1). This is because of the low packing ratio and loss of active biomass by repeating freezing and thawing cycles. Particularly, specific nitrogen conversion rate of anammox bacteria was decreased to 90% after one cycle freezing and thawing in a previous study (Magrı et al., 2012). To overcome these shortcomings, the addition of glycerol is required. The effect of glycerol addition was proven that the death rate of activated sludge and *Escherichia coli* immobilized in a cryoPVAG was minimized by mixing with 4% v/v of glycerol

(Ariga et al., 1987). Therefore, further studies are needed to determine the optimal packing ratio and prevent microbial death by using a protective compound such glycerol.

3.2. Effects of inoculum source

As shown in Table 2, the anammox enrichment process using alternative seeding sources, such as AS from anaerobic digestion, landfill leachate treatment and sewage treatment plants showed long lag periods (Shen et al., 2012; Bae et al., 2015; Gutwinski et al., 2016; Cho et al., 2017; Lu et al., 2018). Particularly, an up-flow column and moving bed biofilm reactors showed the shortest lag periods of 60 and 42 days with packing ratios of 50 and 30%, respectively (Bae et al., 2015; Lu et al., 2018). To overcome the relatively slow increase in anammox activity, the packing ratio of cryoPVAG can be increased. However, increasing the number of flat type cryoPVAG would change the rheology of the bulk phase, possibly reducing the mixing efficiency. Thus, an approach to design the fixed bed reactor configuration using flat type cryoPVAG is required.

In this study, to verify the effects of different seeding sources of AS immobilized in cryoPVAGs, anammox activity of the reactors was analyzed in terms of the lag period and growth rate based on the modified Gompertz model (Fig. 3). The enrichment performance of cryoPVAG according to seeding sludge can be explained by comparing the results of PAB-1mm and AS-1mm. The anammox reaction using cryoPVAG seeded with AS from anoxic phase in A2O (AS-1mm) was initiated at approximately 70 days. The anammox reaction using the PAB-1mm occurred approximately 14 days earlier, and the acceleration of NRR in terms of the R_{max} value of PAB-1mm was 2-fold higher than that of AS-1mm in the modified Gompertz model.

3.3. Effects of cryoPVAG thickness

In an anammox system using granular biomass, the depth at which the substrate can penetrate is approximately 0.8–1.3 mm (Ni et al., 2009; Cho et al., 2010). With respect to the whole cell immobilization system, the growth of anammox bacteria deteriorates the diffusion limitation of substrates through the gel matrix (Leenen et al., 1996; Bae et al., 2015). This problem was solved by reducing the content of PVA; however, this destabilizes the PVA gel structure (Holloway et al., 2013; Ali et al., 2015).

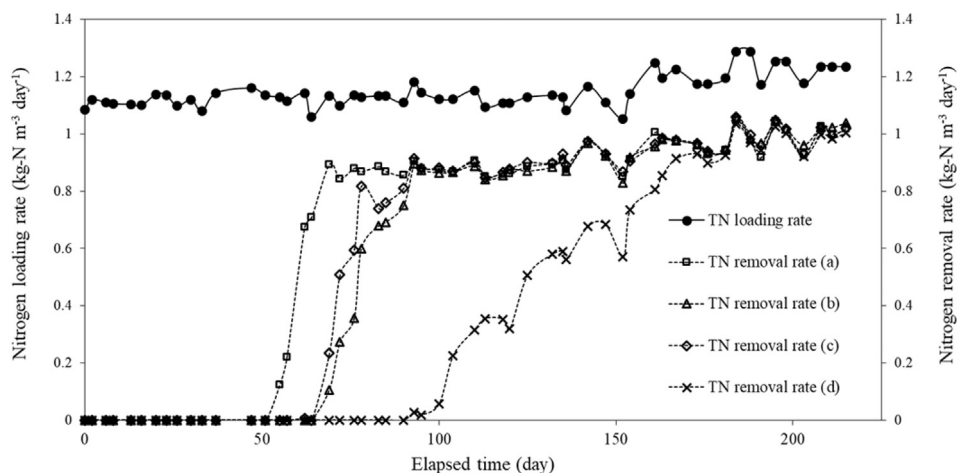


Fig. 1. Temporal profiles of nitrogen loading and removal rate in four reactors. (a) 1 mm thickness of cryoPVAG with PAB inoculum, (b) 1 mm thickness of cryoPVAG with AS inoculum, (c) 2 mm thickness of cryoPVAG with AS inoculum, (d) 3 mm thickness of cryoPVAG with AS inoculum.

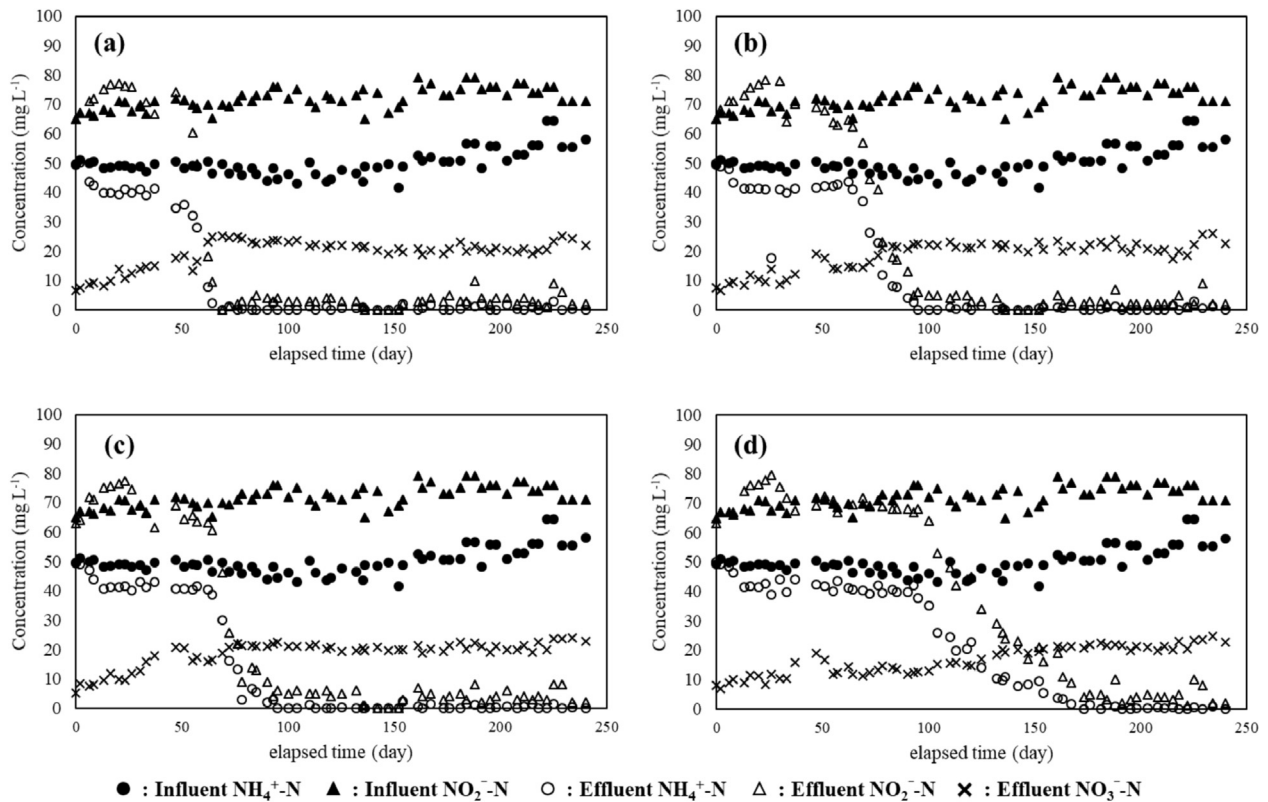


Fig. 2. Transformation profiles of nitrogen compounds in four reactors. (a) 1 mm thickness of cryoPVAG with PAB inoculum, (b) 1 mm thickness of cryoPVAG with AS inoculum, (c) 2 mm thickness of cryoPVAG with AS inoculum, (d) 3 mm thickness of cryoPVAG with AS inoculum.

Table 1

Comparison of start-up period using pre-cultured anammox biomass in different whole cell immobilization system.

NO. Whole cell immobilization technique	Working volume (L)	Lag period (day)	Packing ratio (v/v %)	Initial VSS (g L ⁻¹)	Maximum NRR (kg-N m ⁻³ day ⁻¹)	Reactor type	Reference
1 PVA-SA	2	20	40	17.8	0.6	SBR	(Zhu et al., 2014)
2 PVA-SA	14	9	18.5	0.85	1.5	MBBR	(Cho et al., 2017)
3 PVA-SA	1.0	22	30	16.7	1.0	MBBR	(Quan et al., 2011)
4 PVA-SA	0.01	14	70	1.67	About 10	Up-flow column reactor	(Ali et al., 2015)
5 cryoPVAG	1.4	30	20	11.3	0.58	MBBR	(Magrí et al., 2012)
6 cryoPVAG	0.23	69	1.7	5.3	1.1	FBFR	In this study

Table 2

Comparison of different seeding source for anammox process.

NO. Seeding source	Working volume (L)	Lag period (day)	Initial VSS (g L ⁻¹)	Maximum NRR (kg-N m ⁻³ day ⁻¹)	Reactor type	Reference
1 Landfill leachate plant	2.2	360	17.4	1.91	SBR	(Shen et al., 2012)
2 Municipal sewage treatment plant			12.3	1.10		
3 MSG wastewater treatment plant			17.8	2.85		
4 Municipal wastewater plant	7.85	60	2.0	0.19	Up-flow column reactor	(Lu et al., 2018)
5 CAS + Municipal wastewater plant	50	125	2.97	0.05	AnMBR	(Gutwiński et al., 2016)
6 Anaerobic digestion plant	2	42	14.9	0.78	MBBR (PVA)	(Bae et al., 2015)
7 Anaerobic digestion plant	14	93	9.0	0.4	MBBR (PVA)	(Cho et al., 2017)
8 Anaerobic digestion plant	0.23	93	7.1	1.1	FBFR (PVA)	In this study

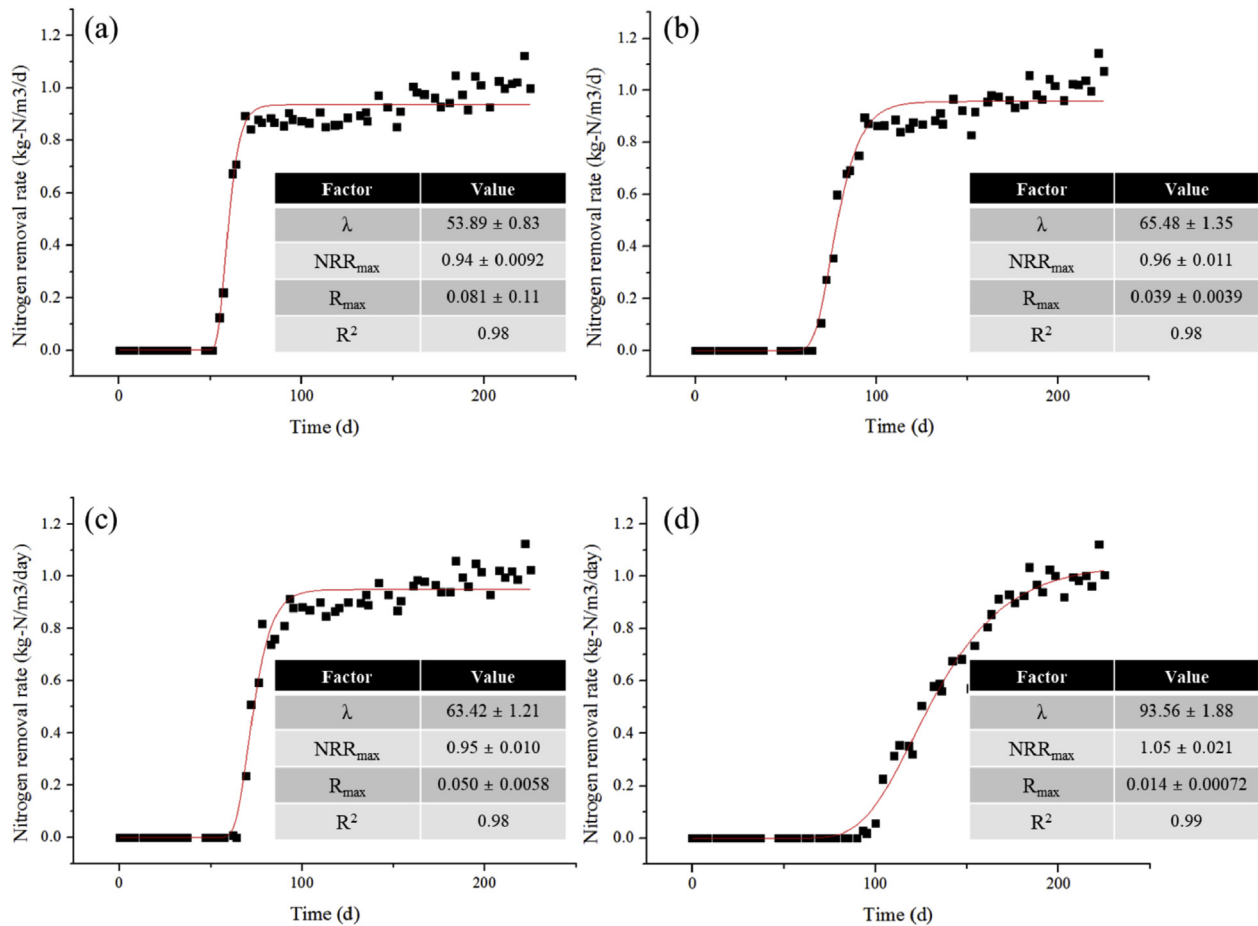


Fig. 3. Modified Gompertz model simulation of four reactor using NRR. (a) 1 mm thickness of cryoPVAG with PAB inoculum, (b) 1 mm thickness of cryoPVAG with AS inoculum, (c) 2 mm thickness of cryoPVAG with AS inoculum, (d) 3 mm thickness of cryoPVAG with AS inoculum.

Furthermore, few studies have examined the depth of substrate diffusion through the cryoPVAG, and the effect of thickness on the lag period was not evaluated. In this study, to evaluate anammox activity according to cryoPVAG thickness, NRRs of AS-1mm, AS-2mm and AS-3mm were compared. As shown in Fig. 3, the lag periods of the anammox reaction (λ) in AS-1mm and AS-2mm were nearly identical (65.48 ± 1.35 and 63.42 ± 1.21 days, respectively); however, the lag period was significantly higher for AS-3mm (93.56 ± 1.88 days). As described above, the elapsed time to reach maximum NRR (R_{max}) for AS-3mm was approximately 3.1-fold longer than those of AS-1mm and AS-2mm. These results indicate that cryoPVAG more than 3 mm in thickness will significantly increase the start-up period of anammox process at a fixed packing ratio because of the dead space. Note that substrates penetrated from both sides, and active thickness was expected to be less than 1.5 mm for AS-3mm.

3.4. Installation of blank cryoPVAG

When the boric acid gelling method for PVA-SA was utilized, floating of the PVA-SA gel occurred because the produced gas was trapped in the gel (Hsia et al., 2008). To solve this problem, the gelling procedure was changed to the repetitive freezing and thawing in this study. As a result, cryoPVAG showed no structural deformation of the cryoPVAG because of efficient gas transport with macroporous heterophase morphology with a variation of thickness less than 0.1 mm (data not shown) (Lozinsky et al., 2008).

These characteristics of cryoPVAG are important beneficial factors as a biocarrier for anammox process.

The flat type cryoPVAG appeared as light red in the PAB reactor and dark black in the AS reactor, depending on the initial type of inoculum. Over time, reddish microorganisms were observed to grow on the gel surface, and simultaneous removal of NH_4^+-N and NO_2^- was detected. Thereafter, reddish anammox bacteria coexisted on the surface of cryoPVAG and in the bulk phase. To identify the contribution of immobilized and suspended anammox bacteria to the NRR, blank cryoPVAGs were installed to eliminate the effect of anammox bacteria immobilized in the cryoPVAGs. The results for the last 15 days, i.e., the last three sampling points in Fig. 1, showed that NRRs were stably maintained with blank cryoPVAG for all bioreactors. These results indicate that the maximum NRR was mostly attributed to the suspended anammox bacteria, while the conditions of inoculum and thickness controlled the lag period. In this sense, the retention of suspended biomass in the immobilized system is an important factor for the NRR. Integrated fixed-film activated sludge (IFAS), the modified moving bed bioreactor (MBBR), is the representative process that simultaneously uses attached and suspended biomass for nitrogen removal (Germain et al., 2007; Veuillet et al., 2014). In the IFAS process, the suspended biomass is returned to the reactor after settling in the subsequent settler, and mixed liquor suspended solids (MLSS) is maintained at a high level (2–5 g-MLSS/L). In this study, similar to the IFAS process, anammox reaction can be maximized through retention of suspended biomass by settling and recycling. To

validate the individual contribution of the fixed and suspended anammox biomass to the NRR, the 16S rRNA gene copy numbers of anammox bacteria were quantified using qPCR for the cryoPVAG and bulk phase, as described below.

3.5. Quantification of total bacteria and anammox bacteria

qPCR analysis was performed to quantify total and anammox

bacteria (Fig. 4). In the initial gel, the 16S rRNA gene of total bacteria using PAB inoculum (PAB-*ini*-gel) and AS inoculum (AS-*ini*-gel) were quantified as $(1.8 \pm 0.12) \times 10^{11}$ and $(1.4 \pm 0.018) \times 10^{11}$ copies, respectively. In the case of anammox bacteria for the same period, the copy numbers were $(8.8 \pm 0.69) \times 10^8$ and $(6.3 \pm 1.8) \times 10^6$ copies, respectively. The 16S rRNA gene copy numbers of anammox bacteria of PAB inoculum were nearly two orders of magnitude higher than that using AS inoculum in the

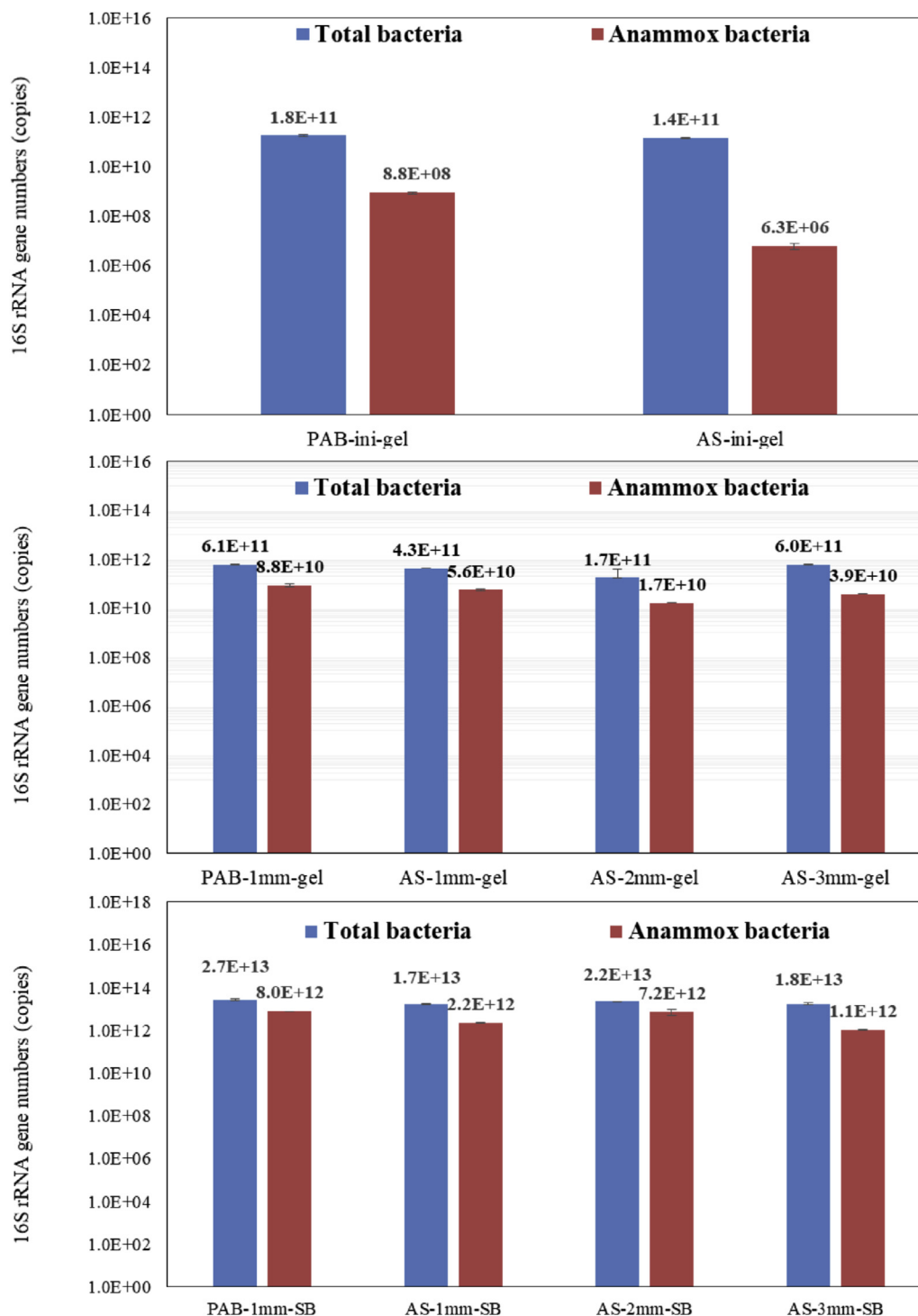


Fig. 4. Real time qPCR results for different reactors with cryoPVAG. (total bacteria (blue bar) and anammox bacteria (red bar)). (For interpretation of the references to colour in this figure legend, the reader is referred to the Web version of this article.)

initial cryoPVAG sample. This large difference in the bacterial population resulted in a different lag period of anammox enrichment using the PAB and AS inoculum. However, different inoculum sources provided little effect on bacterial growth.

After the completion of anammox enrichment, qPCR was performed for the cryoPVAGs (PAB-1mm-gel, AS-1mm-gel, AS-2mm-gel and AS-3mm-gel) and SB (PAB-1mm-SB, AS-1mm-SB, AS-2mm-SB and AS-3mm-SB). Under the four conditions, the 16S rRNA gene of total bacteria in cryoPVAGs was quantified as $(6.1 \pm 0.24) \times 10^{11}$, $(4.3 \pm 0.075) \times 10^{11}$, $(1.7 \pm 2.2) \times 10^{11}$ and $(6.0 \pm 0.36) \times 10^{11}$ copies, respectively. In the same location, the copy numbers of anammox bacteria were $(8.8 \pm 1.3) \times 10^{10}$, $(5.6 \pm 0.29) \times 10^{10}$, $(1.7 \pm 0.031) \times 10^{10}$, and $(3.9 \pm 0.16) \times 10^{10}$ copies, respectively. Even though different inoculum sources had effects on anammox growth at the initial phase, fully enriched anammox growth may have not been affected regardless of inoculum sources and gel thicknesses. The resulting copy numbers were considered as the saturated value within the cryoPVAG.

In the case of SB, the 16S rRNA gene of total bacteria was quantified as $(2.7 \pm 0.26) \times 10^{13}$, $(1.7 \pm 0.14) \times 10^{13}$, $(2.2 \pm 0.078) \times 10^{13}$ and $(1.8 \pm 0.18) \times 10^{13}$ copies for PAB-1mm, AS-1mm, AS-2mm and AS-3mm, respectively. The copy numbers of anammox bacteria were smaller by one order of magnitude than those of total bacteria with values of $(8.0 \pm 0.037) \times 10^{12}$, $(2.2 \pm 0.094) \times 10^{12}$, $(7.2 \pm 2.0) \times 10^{12}$ and $(1.1 \pm 0.054) \times 10^{12}$ copies, respectively. In each reactor, compared to those of cryoPVAG in the attached growth phase, the total and anammox bacteria in the suspended growth phase were approximately 100 times more abundant. These findings suggest that the observed anammox activities might have been attributed to the suspended grown microbes detached from the solid gel phase.

3.6. Microbial community characteristics

Illumina MiSeq sequencing was performed to characterize the bacterial community structure. Valid reads, OTUs and alpha diversity results at distance cutoff level of 0.03 in each sample are shown Table S4. A total of 1,343,245 reads and 1725 OTUs were detected from 10 samples. The reads and OTUs of each reactor were 69,272–244,500 and 107–292, respectively. The estimated Shannon index values showed a tendency to decrease in both the mature cryoPVAG and SB samples after the anammox enrichment compared to the initial cryoPVAG samples, regardless of the different inoculum sources. The decreased bacterial diversity indicates that the mature cryoPVAG and SB microbes were selectively enriched.

A 2D ordination plot (Fig. 5a) was used to compare the microbial communities of each reactor. The results indicate that the structure of microbial community could be divided into three group; initial two samples of cryoPVAGs (PAB-ini-gel and AS-ini-gel) and other samples (cryoPVAGs and suspended biomass after anammox reaction). A hierarchical clustering dendrogram (Fig. 5b) also showed that the first branch formed the initial cryoPVAG using AS inoculum, while the second branch was constructed by initial cryoPVAG with PAB inoculum. Based on the results for the cryoPVAG and SB samples after the anammox reaction, samples with a thickness of 3 mm were separated in the dendrogram. The following branch showed that the cryoPVAG and SB samples after the anammox reaction were clustered in a similar position and not considerably different. These results suggest that microbial communities were initially affected by different inoculum sources. After the anammox reaction, microbial community structures were similar to each other because the reactors were operated with the same substrate and under the same operational conditions. Nevertheless, as the gel thickness increased, the penetration of the substrate into the

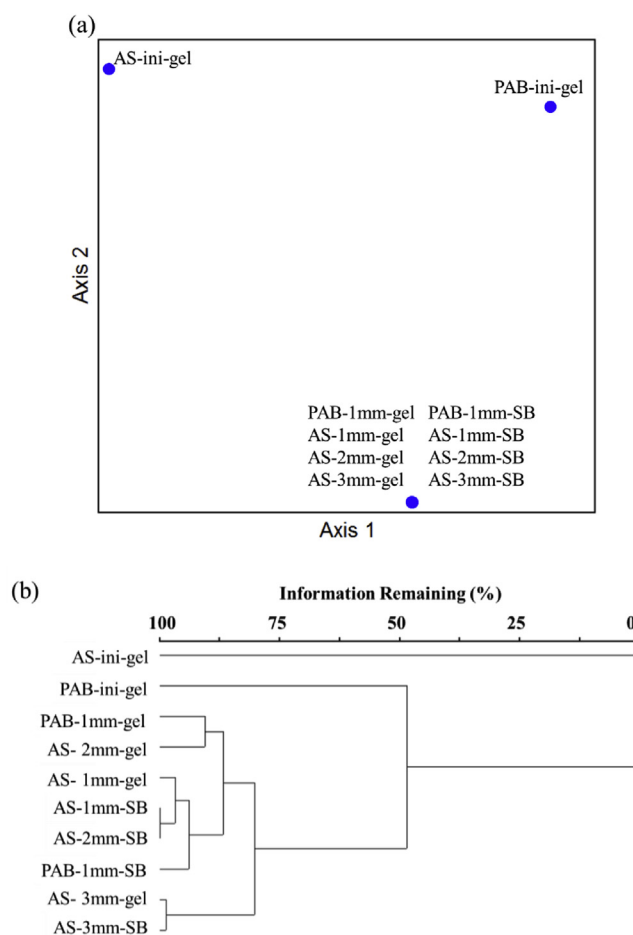


Fig. 5. (a) 2D ordination plot and (b) dendrogram of correspondence analysis for samples of different reactor based on Illumina miseq results.

internal space may have been restricted, slowing the rate at which the bacterial community structure was unified.

3.7. Taxonomic composition

Fig. 6 shows the OTU distribution of the bacterial community in all four reactors. Detailed microbial community analysis of the genus level is shown in Table S5. In the initial cryoPVAG sample

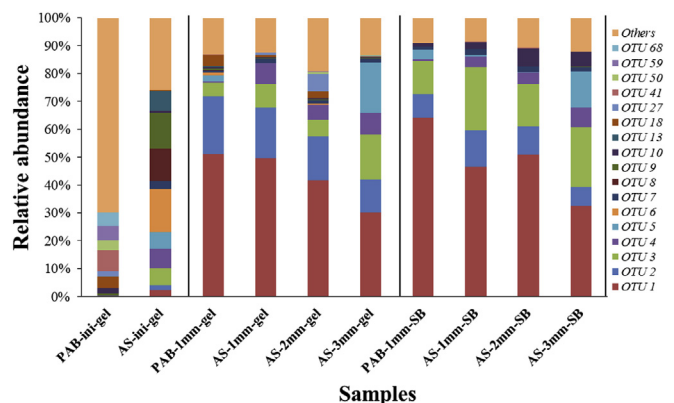


Fig. 6. Relative abundance of the OTUs using Illumina miseq in the different cryoPVAG samples.

with PAB inoculum, the most dominant genus was *Dokdonella kunshanensis* (OTU 6, 15.4%) which is known to be present in the activated sludge of sewage treatment plants (Jahan et al., 2013). In the case of anammox microorganisms, *Candidatus Jettenia asiatica* (OTU 13) was detected with a relative abundance of 7.3%. In contrast, various microbial communities were found in initial cryoPVAG using AS inoculum. *Candidatus Nitrospira defluvii* (OTU 41, 7.4%) of the nitrite-oxidizing bacterium was most commonly found in the initial cryoPVAG samples, while no microbial species associated with anammox bacteria were detected.

After anammox enrichment, the most abundant microorganism was *Candidatus Brocadia sinica* (OTU 1) in both cryoPVAG and SB samples under all gelation conditions. Neutral pH (7.5–8) and low salinity are suitable conditions for the growth of *Candidatus Brocadia sinica* (Oshiki et al., 2015). Therefore, in the anammox reaction, the growth of *Candidatus Brocadia sinica* was maximized using the artificial medium with tap water. The proportion of *Candidatus Brocadia sinica* in the total microbial communities was highest in the cryoPVAG sample using the PAB inoculum. In case of cryoPVAG samples with AS inoculum, the ratio was similar at 1 mm and 2 mm, but decreased sharply at 3 mm.

Candidatus Jettenia asiatica was found in the anammox consortium of the PAB inoculum, however, *Candidatus Brocadia sinica* predominated the bacterial community after the enrichment. Based on physiological properties, “*Candidatus Brocadia*” has a higher maximum specific growth rate and shows better resistance to nitrite than “*Candidatus Jettenia*” (Oshiki et al., 2016; Zhang et al., 2017). Therefore, cryoPVAG containing a high abundance of *Candidatus Brocadia sinica* is useful to treat nitrogen in high NLR conditions.

4. Conclusion

Anammox enrichment with cryoPVAG using different inoculum sources (PAB and AS) and gel thicknesses (1, 2 and 3 mm) was successfully performed at an NLR of $1 \text{ kg-N m}^{-3} \text{ day}^{-1}$. The inoculum source and thickness affected the start-up period, but maximum NRR values were similar. The late start-up period with the 3-mm-thick gel was attributed to substrate diffusion limitation in the cryoPVAG. qPCR results showed that suspended anammox biomass in the bulk phase, which originally detached from the cryoPVAG, mostly contributed to the NRR. The results of Illumina MiSeq indicated that *Candidatus Brocadia sinica* was responsible for the anammox reaction.

Acknowledgements

This work was supported by the Korea Institute of Science and Technology (2E27102) and the National Research Foundation of Korea grant funded by the Korea government (MSIP) (No. 2011-0030040).

Appendix A. Supplementary data

Supplementary data related to this article can be found at <https://doi.org/10.1016/j.chemosphere.2018.04.055>.

References

Ali, M., Oshiki, M., Rathnayake, L., Ishii, S., Satoh, H., Okabe, S., 2015. Rapid and successful start-up of anammox process by immobilizing the minimal quantity of biomass in PVA-SA gel beads. *Water Res.* 79, 147–157.

Ariga, O., Takagi, H., Nishizawa, H., Sano, Y., 1987. Immobilization of microorganisms with PVA hardened by iterative freezing and thawing. *J. Ferment. Technol.* 65, 651–658.

Asano, H., Myoga, H., Asano, M., Toyao, M., 1992. A study of nitrification utilizing

whole microorganisms immobilized by the PVA-freezing method. *Water Sci. Technol.* 26, 1037–1046.

Bae, H., Choi, M., Chung, Y.-C., Lee, S., Yoo, Y.J., 2017. Core-shell structured poly (vinyl alcohol)/sodium alginate bead for single-stage autotrophic nitrogen removal. *Chem. Eng. J.* 322, 408–416.

Bae, H., Choi, M., Lee, C., Chung, Y.-C., Yoo, Y.J., Lee, S., 2015. Enrichment of ANAMMOX bacteria from conventional activated sludge entrapped in poly (vinyl alcohol)/sodium alginate gel. *Chem. Eng. J.* 281, 531–540.

Bae, H., Chung, Y.-C., Jung, J.-Y., 2010a. Microbial community structure and occurrence of diverse autotrophic ammonium oxidizing microorganisms in the anammox process. *Water Sci. Technol.* 61, 2723–2732.

Bae, H., Park, K.-S., Chung, Y.-C., Jung, J.-Y., 2010b. Distribution of anammox bacteria in domestic WWTPs and their enrichments evaluated by real-time quantitative PCR. *Process Biochem.* 45, 323–334.

Bae, H., Paul, T., Kim, D., Jung, J.-Y., 2016. Specific ANAMMOX activity (SAA) in a sequencing batch reactor: optimization test with statistical comparison. *Environ. Earth Sci.* 75, 1452.

Chen, K.-C., Chen, S.-J., Hwang, J.-Y., 1996. Improvement of gas permeability of denitrifying PVA gel beads. *Enzym. Microb. Technol.* 18, 502–506.

Chen, K.-C., Hwang, J.-Y., 1997. Cell immobilization with phosphorylated polyvinyl alcohol (PVA) gel. In: Bickerstaff, G.F. (Ed.), *Immobilization of Enzymes and Cells*. Humana Press, Totowa, NJ, pp. 207–216.

Chen, K.-C., Lin, Y.-F., 1994. Immobilization of microorganisms with phosphorylated polyvinyl alcohol (PVA) gel. *Enzym. Microb. Technol.* 16, 79–83.

Cho, K., Choi, M., Jeong, D., Lee, S., Bae, H., 2017. Comparison of inoculum sources for long-term process performance and fate of ANAMMOX bacteria niche in poly (vinyl alcohol)/sodium alginate gel beads. *Chemosphere* 185, 394–402.

Cho, S., Takahashi, Y., Fujii, N., Yamada, Y., Satoh, H., Okabe, S., 2010. Nitrogen removal performance and microbial community analysis of an anaerobic up-flow granular bed anammox reactor. *Chemosphere* 78, 1129–1135.

Chou, W., Tseng, S., Ho, C., 2012. Anaerobic ammonium oxidation improvement via a novel capsule bioreactor. *Environ. Technol.* 33, 2105–2110.

Egli, K., Fanger, U., Alvarez, P.J., Siegrist, H., van der Meer, J.R., Zehnder, A.J., 2001. Enrichment and characterization of an anammox bacterium from a rotating biological contactor treating ammonium-rich leachate. *Arch. Microbiol.* 175, 198–207.

Fux, C., Marchesi, V., Brunner, I., Siegrist, H., 2004. Anaerobic ammonium oxidation of ammonium-rich waste streams in fixed-bed reactors. *Water Sci. Technol.* 49, 77–82.

Germain, E., Bancroft, L., Dawson, A., Hinrichs, C., Fricker, L., Pearce, P., 2007. Evaluation of hybrid processes for nitrification by comparing MBBR/AS and IFAS configurations. *Water Sci. Technol.* 55, 43–49.

Gutwiński, P., Cema, G., Ziemińska-Buczyńska, A., Surmacz-Górska, J., Osadnik, M., 2016. Startup of the anammox process in a membrane bioreactor (AnMBR) from conventional activated sludge. *Water Environ. Res.* 88, 2268–2274.

Holloway, J.L., Lowman, A.M., Palmese, G.R., 2013. The role of crystallization and phase separation in the formation of physically cross-linked PVA hydrogels. *Soft Matter* 9, 826–833.

Hsia, T.-H., Feng, Y.-J., Ho, C.-M., Chou, W.-P., Tseng, S.-K., 2008. PVA-alginate immobilized cells for anaerobic ammonium oxidation (anammox) process. *J. Ind. Microbiol. Biotechnol.* 35, 721–727.

Isaka, K., Sumino, T., Tsuneda, S., 2007. High nitrogen removal performance at moderately low temperature utilizing anaerobic ammonium oxidation reactions. *J. Biosci. Bioeng.* 103, 486–490.

Jahan, K., Hoque, S., Ahmed, T., 2013. Activated sludge and other aerobic suspended culture processes. *Water Environ. Res.* 85, 992–1059.

Jin, R.-C., Zhang, Q.-Q., Yang, G.-F., Xing, B.-S., Ji, Y.-X., Chen, H., 2013. Evaluating the recovery performance of the ANAMMOX process following inhibition by phenol and sulfide. *Bioresour. Technol.* 142, 162–170.

Jin, R.-C., Zheng, P., Hu, A.-H., Mahmood, Q., Hu, B.-L., Jilani, G., 2008. Performance comparison of two anammox reactors: SBR and UBF. *Chem. Eng. J.* 138, 224–230.

Klindworth, A., Pruesse, E., Schweer, T., Peplies, J., Quast, C., Horn, M., Glöckner, F.O., 2013. Evaluation of general 16S ribosomal RNA gene PCR primers for classical and next-generation sequencing-based diversity studies. *Nucleic Acids Res.* 41, e1.

Kowalchuk, G.A., de Bruijn, F.J., Head, I.M., Akkermans, A.D., van Elsas, J.D., 2004. Section 7-Statistical, computer-assisted and other analyses. In: Kowalchuk, G.A., de Bruijn, F.J., Head, I.M., Akkermans, A.D., van Elsas, J.D. (Eds.), *Molecular Microbial Ecology Manual*. Springer Netherlands, Dordrecht, pp. 1319–1560.

Leenen, E.J., Dos Santos, V.A., Grolle, K.C., Tramper, J., Wijffels, R., 1996. Characteristics of and selection criteria for support materials for cell immobilization in wastewater treatment. *Water Res.* 30, 2985–2996.

Lozinsky, V., Damshkahn, L., Kurochkin, I., Kurochkin, I., 2008. Study of cryostructuring of polymer systems: 28. Physicochemical properties and morphology of poly (vinyl alcohol) cryogels formed by multiple freezing-thawing. *Colloid J.* 70, 189–198.

Lozinsky, V.I., Galaev, I.Y., Plieva, F.M., Savina, I.N., Jungvid, H., Mattiasson, B., 2003. Polymeric cryogels as promising materials of biotechnological interest. *Trends Biotechnol.* 21, 445–451.

Lozinsky, V.I., Okay, O., 2014. Basic principles of cryotropic gelation. In: Okay, O. (Ed.), *Polymeric Cryogels: Macroporous Gels with Remarkable Properties*. Springer International Publishing, Cham, pp. 49–101.

Lu, Y.-F., Ma, L.-J., Ma, L., Shan, B., Chang, J.-J., 2018. Improvement of start-up and nitrogen removal of the anammox process in reactors inoculated with

- conventional activated sludge using biofilm Carrier materials. *Environ. Technol.* 39, 59–67.
- Magri, A., Vanotti, M.B., Szögi, A.A., 2012. Anammox sludge immobilized in polyvinyl alcohol (PVA) cryogel carriers. *Bioresour. Technol.* 114, 231–240.
- Mulder, A., Van de Graaf, A.A., Robertson, L., Kuenen, J., 1995. Anaerobic ammonium oxidation discovered in a denitrifying fluidized bed reactor. *FEMS Microbiol. Ecol.* 16, 177–183.
- Nadkarni, M.A., Martin, F.E., Jacques, N.A., Hunter, N., 2002. Determination of bacterial load by real-time PCR using a broad-range (universal) probe and primers set. *Microbiology* 148, 257–266.
- Ni, B.J., Chen, Y.P., Liu, S.Y., Fang, F., Xie, W.M., Yu, H.Q., 2009. Modeling a granule-based anaerobic ammonium oxidizing (ANAMMOX) process. *Biotechnol. Bioeng.* 103, 490–499.
- Oshiki, M., Satoh, H., Okabe, S., 2016. Ecology and physiology of anaerobic ammonium oxidizing bacteria. *Environ. Microbiol.* 18, 2784–2796.
- Oshiki, M., Shinyako-Hata, K., Satoh, H., Okabe, S., 2015. Draft genome sequence of an anaerobic ammonium-oxidizing bacterium, “*Candidatus Brocadia sinica*”. *Genome Announc.* 3 e00267–00215.
- Quan, L.M., Hira, D., Fujii, T., Furukawa, K., 2011. Reject water treatment by improvement of whole cell anammox entrapment using polyvinyl alcohol/alginate gel. *Biodegradation* 22, 1155–1167.
- Shen, L.-d., Hu, A.-h., Jin, R.-c., Cheng, D.-q., Zheng, P., Xu, X.-y., Hu, B.-l., 2012. Enrichment of anammox bacteria from three sludge sources for the startup of monosodium glutamate industrial wastewater treatment system. *J. Hazard Mater.* 199–200, 193–199.
- Sheng, P.X., Wee, K.H., Ting, Y.P., Chen, J.P., 2008. Biosorption of copper by immobilized marine algal biomass. *Chem. Eng. J.* 136, 156–163.
- Smith, V.H., Tilman, G.D., Nekola, J.C., 1999. Eutrophication: impacts of excess nutrient inputs on freshwater, marine, and terrestrial ecosystems. *Environ. Pollut.* 100, 179–196.
- Strous, M., Heijnen, J., Kuenen, J.G., Jetten, M., 1998. The sequencing batch reactor as a powerful tool for the study of slowly growing anaerobic ammonium-oxidizing microorganisms. *Appl. Microbiol. Biotechnol.* 50, 589–596.
- Tang, Y., Pang, L., Wang, D., 2017. Preparation and characterization of borate bioactive glass cross-linked PVA hydrogel. *J. Non-Cryst. Solids* 476, 25–29.
- Tian, Z., Zhang, J., Song, Y., 2015. Several key factors influencing nitrogen removal performance of anammox process in a bio-filter at ambient temperature. *Environ. Earth Sci.* 73, 5019–5026.
- Trigo, C., Campos, J., Garrido, J., Mendez, R., 2006. Start-up of the Anammox process in a membrane bioreactor. *J. Biotechnol.* 126, 475–487.
- Van de Graaf, A.A., Mulder, A., de Bruijn, P., Jetten, M., Robertson, L.A., Kuenen, J.G., 1995. Anaerobic oxidation of ammonium is a biologically mediated process. *Appl. Environ. Microbiol.* 61, 1246–1251.
- Van Dongen, U., Jetten, M.S., Van Loosdrecht, M., 2001. The SHARON®-Anammox® process for treatment of ammonium rich wastewater. *Water Sci. Technol.* 44, 153–160.
- Veuillet, F., Lacroix, S., Bausseron, A., Gonidec, E., Ochoa, J., Christensson, M., Lemaire, R., 2014. Integrated fixed-film activated sludge ANITA™ Mox process—a new perspective for advanced nitrogen removal. *Water Sci. Technol.* 69, 915–922.
- Yamamoto, T., Takaki, K., Koyama, T., Furukawa, K., 2008. Long-term stability of partial nitrification of swine wastewater digester liquor and its subsequent treatment by Anammox. *Bioresour. Technol.* 99, 6419–6425.
- Zhang, L., Narita, Y., Gao, L., Ali, M., Oshiki, M., Okabe, S., 2017. Maximum specific growth rate of anammox bacteria revisited. *Water Res.* 116, 296–303.
- Zhang, Y., Ye, L., 2011. Improvement of permeability of poly (vinyl alcohol) hydrogel by using poly (ethylene glycol) as porogen. *Polym. Plast. Technol. Eng.* 50, 776–782.
- Zhu, G.-L., Yan, J., Hu, Y.-Y., 2014. Anaerobic ammonium oxidation in polyvinyl alcohol and sodium alginate immobilized biomass system: a potential tool to maintain anammox biomass in application. *Water Sci. Technol.* 69, 718–726.